Indian Journal of Pure & Applied Physics
Vol. 64, January 2026, pp. 18-28
DOI: 10.56042/ijpap.v64i1.20475

Circuit Model Equivalent for Load-Based Discharge of Supercapacitor Module

Aditya S Sengupta[a], Nikhat Anjum[b], Bidyut K Bhattacharyya[c], Mukesh Kumar Ojha[d], Shaik Qadeer[e] & Vijay Nath[b*]

[a]Department of Electrical and Electronics Engineering, FST, ICFAI University Tripura, Kamalghat 799 210, India

[b]Department of Electronics and Communication Engineering, Birla Institute of Technology, Mesra 835 215, India

[c]Department of Electronics and Communication Engineering, National Institute of Technology, Agartala 799 046, India

[d]Department of Electronics and Communication Engineering, Institute of Technology, Greater Noida 201 310, India

[e]Department of Electrical Engineering, Muffakham Jah College of Engineering and Technology, Hyderabad 500 034, India

Received: 9th June 2025; accepted:16th December 2025

The discharge behaviour of the Supercapacitor module (SCM) when it supplies a certain load is simulated. In scenario 1, a constant power application is powered by the SCM via a buck circuit, resulting in a constant output voltage. The voltage of the SCM will decay depending on the power drawn by the application and the different components of the circuit. The constant output voltage is obtained from the buck circuit by using a control circuit that will change the duty ratio as a function of the SCM voltage. The output remains unaffected by current changes from 450 mA to 1.2 A. The decay characteristics of SCM, including duty ratio and output voltage, are recorded. In scenario 2, another buck topology is designed that generates a decaying voltage from a power supply, almost like the voltage of the SCM. This circuit is used to power the same DC application via a DC-DC converter, and the respective decaying voltage, output voltage, and other parameters have been recorded. The simulation results from both scenarios have been tallied, leading to the inference that the circuit in scenario 2 can be used as an alternative to SCM for DC applications, and the successful operation time, a probable characteristic of SCM, can be estimated.

Keywords: Supercapacitor, Module, Discharge, Converter, Model

1 Introduction

Renewable energy has gained considerable momentum in recent years[1-2]. The use of supercapacitors in the field of renewable energy has become extensive, to the extent that supercapacitor technology is also utilised in renewable-based electric vehicle applications[3-5]. Even rural applications are catering to the use of renewable energy systems for storing energy generated from renewable sources. different energy storage systems like double-layered capacitors, batteries, and fuel cells are used, and these energy storage systems play an important role in this field[6-11]. As the use of supercapacitors has become widespread, they have recently become a preferred choice for energy storage in the field of energy[12].

Supercapacitors, often referred to as electrochemical double-layer capacitors (EDLC), were invented by scientists and patented in 1957 for use in recent technologies[13-14]. This supercapacitor technology is advantageous due to its short charging time, which has led to an increase in the number of applications associated with this technology[15-16]. Supercapacitor technology, to some extent, outperforms other existing technologies, such as battery technology. Therefore, several battery-powered applications are integrating supercapacitors into their designs[17-18]. Supercapacitors have a very high-power density, allowing them to supply the instantaneous power required for sudden changes in current, thereby facilitating the simultaneous balancing of fast-changing power surges[19-20]. Most high-capacity supercapacitors available on the market have a very low terminal voltage. Therefore, a supercapacitor module, achieved by connecting a series-parallel combination of supercapacitors, is required for applications that require higher voltage and higher capacitance. Mega Farad Supercapacitors have also been designed to compensate for the high capacitance requirement[21]. It is quite evident from a prior article that charging supercapacitors is an efficient process and can increase the lifetime of applications[22]. Combined with its fast-charging capabilities, it supersedes other energy storage technologies in terms of powering different applications. The voltage from the SCM decays over time. Therefore, the power from supercapacitors is delivered via a DC-DC converter[23-24].

*Corresponding author: E-mail: vijaynath@bitmesra.ac.in

The selection of a converter is purely application-specific, which determines whether a step-up or step-down topology should be used[25-26].

The availability of supercapacitors, depending on the voltage and capacitance required by a specific application, poses a significant challenge, along with the cost per unit. Hence, the formulation of a circuit equivalent to the discharge characteristics of SCM has become compulsory. Such a circuit equivalent could help predict the successful operation time of a device intended to be powered by SCM by using the equivalent circuit model in place of the SCM to power that device.

A constant current drawing application, such as a constant power device like an LED table light, is powered by the SCM via a DC-DC converter circuit[27]. The input from the SCM is a voltage decreasing with time. Hence, a PWM control strategy is used in the design. This control scheme will vary the duty ratio (D) as a function of the decreasing SCM voltage, thereby delivering a constant voltage as required by the application[28-30].

To design the control loop of the converter, articles have been reviewed regarding the operation of the DC-DC converter in continuous conduction mode and discontinuous conduction mode[31-33]. Then, the converter topology for transferring power from the SCM to the application was designed. This converter topology can tolerate output current fluctuations from 450 mA to 1.2 A.

Now, the circuit equivalent of the SCM will be used to supply the application via the DC-DC converter. The voltage profile of the circuit equivalent for SCM is recorded and compared with the discharge profile of SCM when it powers the application via the DC-DC converter to verify the proof of concept.

Even if the approximate power consumption for the application to be supplied by SCM is known, the rate of voltage decay of SCM can be determined. According to this data, a circuit equivalent to simulate SCM's voltage characteristic can be synthesised using a DC-DC converter powered by a DC supply. Such a circuit equivalent should help predetermine the approximate operation time for an application powered by SCM. The SCM referred to in this work has a capacitance of 850 F and a voltage of 11.6V. It is made from a series combination of four identical supercapacitor cells, each with a capacitance of 3400 F and a voltage of 2.9V.

2 Literature Review

Different double-layer capacitors (DLCs) with varying equivalent series resistances (ESR) have been utilised, and a formula to calculate the equivalent parallel resistance (EPR) of the supercapacitor has been presented[34-35]. A MOSFET-based test circuit has been employed to verify their ESR values. Then, the discharge characteristic was plotted by experimenting with these DLCs on a resistive load; also, an RC series-parallel equivalent model for these DLCs was shown. However, the equivalent model hasn't been used to power the same load to verify the discharge characteristic of DLC. Super capacitors with capacitance values of 470 F, 900 F, and 1500 F, and a voltage of 2.3V, have been used. The RC model for DLC has been demonstrated, in which the 'R' and 'C' values of the branches have been determined. However, the model is only said to behave accurately for 30 minutes, after which it becomes less accurate. In a different specification, supercapacitors are used to form two distinct modules for power electronic and transportation-based applications. Experiments have been conducted using these SCMs, and an RC network-based equivalent for SCM has been proposed, in which the values of different resistances and capacitances have been shown to be dependent on the temperature of the SCM in the application. However, the equivalent circuit established has not been used in any application as a replacement for SCM. An equivalent circuit for a supercapacitor has been designed, which is only applicable to porous electrode supercapacitors. This circuit equivalent is an RC ladder network. But this circuit equivalent is only used to generate self-discharge behaviour and not the discharge behaviour based on load. An equivalent circuit for supercapacitors based on a multibranch RC network has been demonstrated, and the 'R' and 'C' values of the equivalent circuit have been determined experimentally. Then, using these values, the final equivalent circuit for the supercapacitor was simulated in MATLAB; however, the circuit has not been used to power any application in place of the supercapacitor to verify the accuracy of the equivalent circuit[36-37]. A two-branch RC model for supercapacitors has been formulated, and the different parameters have been identified through mathematical modelling and experimentation. However, this equivalent model for supercapacitors is said to be valid only in the short term, after which the accuracy of the model cannot be guaranteed[38-39]. A three-branch equivalent model for supercapacitors has been formulated based on the charging and discharging of a commercially available supercapacitor[40-41]. The study of the charging and discharging cycle reveals that the different parameters of this equivalent model are temperature dependent. However, this model has not

been used as a replacement for a supercapacitor to power any application. The different parameters of the circuit equivalent for a supercapacitor have been modelled based on the self-discharge of the supercapacitor, and a final mathematical circuit model of the supercapacitor has been formulated using Electrochemical Impedance Spectroscopy and integration with Lab view software. However, this equivalent model for supercapacitors has not been verified by using it to supply any application[42-44]. A MATLAB-based equivalent model for a supercapacitor has been generated based on its self-discharge, with the aim of using it for wireless sensor nodes. However, no circuit-based practical equivalent model for a supercapacitor has been provided, which could be used in place of a supercapacitor to power any application[45-46]. An RC network-based equivalent model for ultracapacitors has been proposed, and the values of different parameters have been tabulated for different temperatures. Then, a MATLAB-based behavioural model of the ultracapacitor was used, based on which an experiment was also conducted; however, no experimental validation was provided by using the equivalent model to power any application. Two different RC-based equivalent models for 'charging supercapacitor' and 'discharging supercapacitors have been presented for varying loads. In both models, the current through the EPR is an exponential function of the voltage across the EPR. These models haven't been experimentally verified under constant power draw conditions, where the application to be powered by the supercapacitor requires a constant power at a specific voltage level, below which the application would cease to function[47-48].

3 Material and Methods

3.1 SCM Powering Constant Power Application

In Fig. 1, a constant power application, represented by a current source 'Io', is powered by SCM via a buck circuit.

'V_{SCM}' and 'C_{SCM}' are the voltage and equivalent capacitance of the SCM. The MOSFET 'M', Schottky diode 'S', inductor 'L' and capacitor 'C' together constitute the buck converter. 'RL' and 'RC' are the equivalent series resistance (ESR) of L and C, respectively. 'Z1' is a Zener diode[49-51]. 'Vo' is the output voltage of the buck converter that is powering the application drawing constant current 'Io'. 'A1' and 'A2' are identical op-amp.

The part of the circuit inside the black dotted border is the PWM control circuit of the buck converter. The function of this part of the circuit is to change the duty ratio of the switching pulse generated at point 'E' in proportion to the decrease in the value of 'V_{SCM}' over time. This control circuit consists of two parts: the voltage regulator and a sawtooth wave

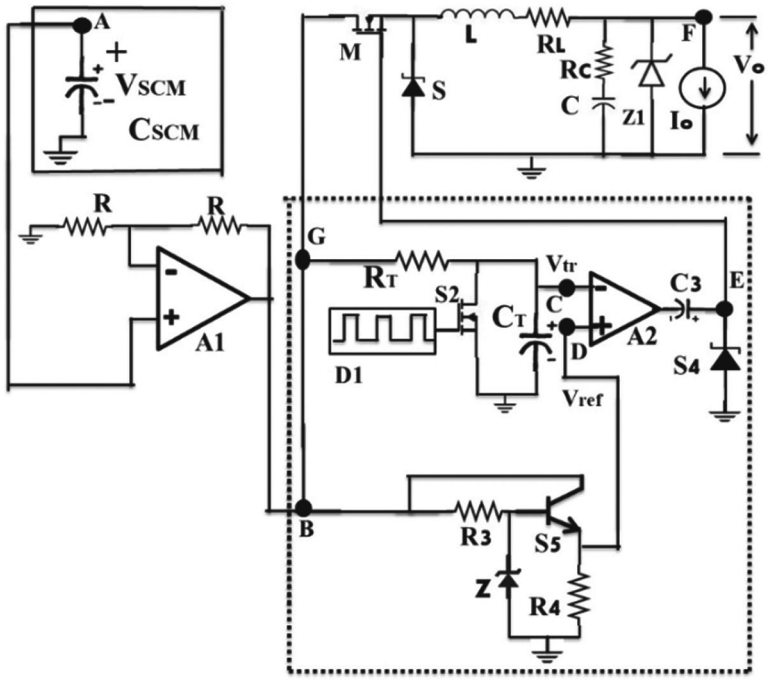

Fig. 1 — Buck Converter Powering Application from SCM

generator, both of which are coupled with a clamper circuit. The voltage regulator is made of resistance 'R3', transistor 'S5', resistance 'R4', and Zener diode 'Z'. The sawtooth wave generator circuit is made of resistance 'R_T', capacitance 'C_T', and MOSFET[52] 'S2', which is operated by a switching pulse of duty ratio 'D1'. The output of 'A1' is almost equal to $2V_{SCM,}$ which will be fed to the points' B' and 'G'.

'V_{SCM}' supplied by the supercapacitor module will decay with time. A sawtooth wave of peak voltage 'V_{tr}' varying as a function of 'V_{SCM}' will be generated at point 'C' by the sawtooth wave generator. A constant reference voltage 'V_{ref}' will be generated at point 'D' via the voltage regulator circuit. The op-amp 'A2' will compare the reference voltage at 'D' and the sawtooth voltage at 'C' to generate a bipolar pulse, the duty ratio of which will keep changing with the changing value of 'V_{SCM}'. The bipolar wave generated at the output of 'A2' will be converted into a unipolar switching pulse by the circuit comprising capacitor 'C3' and Schottky diode 'S5'. And in this manner, a switching pulse whose duty ratio will change as a function of 'V_{SCM}', will be generated at point 'E'. This switching pulse will operate the MOSFET 'M' and, combined with the input from point G', a constant output 'Vo' will be generated at 'F' which will supply the constant power needed by the application.

3.2 Circuit Equivalent for SCM Powering Application

In Fig. 2, the circuit diagram is shown for the circuit equivalent for SCM discharge powering a constant power application via a buck converter.

The part of the circuit inside the black dashed line border is the circuit equivalent for the discharge of SCM, while the rest of the circuit is the same circuit as that shown in Fig. 1. So, in the entire circuit, the circuit equivalent for SCM is used to supply the constant power application via the buck circuit.

'V_i' is the voltage of the power supply, and it is used as the power source for a buck converter made of MOSFET 'M1', Schottky diode 'S1', inductor 'L_1', capacitor 'C1', and Zener diode 'Z1'. 'R_{L1}' and 'R_{C1}' are the ESR values for the inductance and capacitance, respectively. The output of the circuit inside the black dashed border, i.e., at the point 'A', should give us the voltage decay profile of SCM when it is supplying the constant power application via the

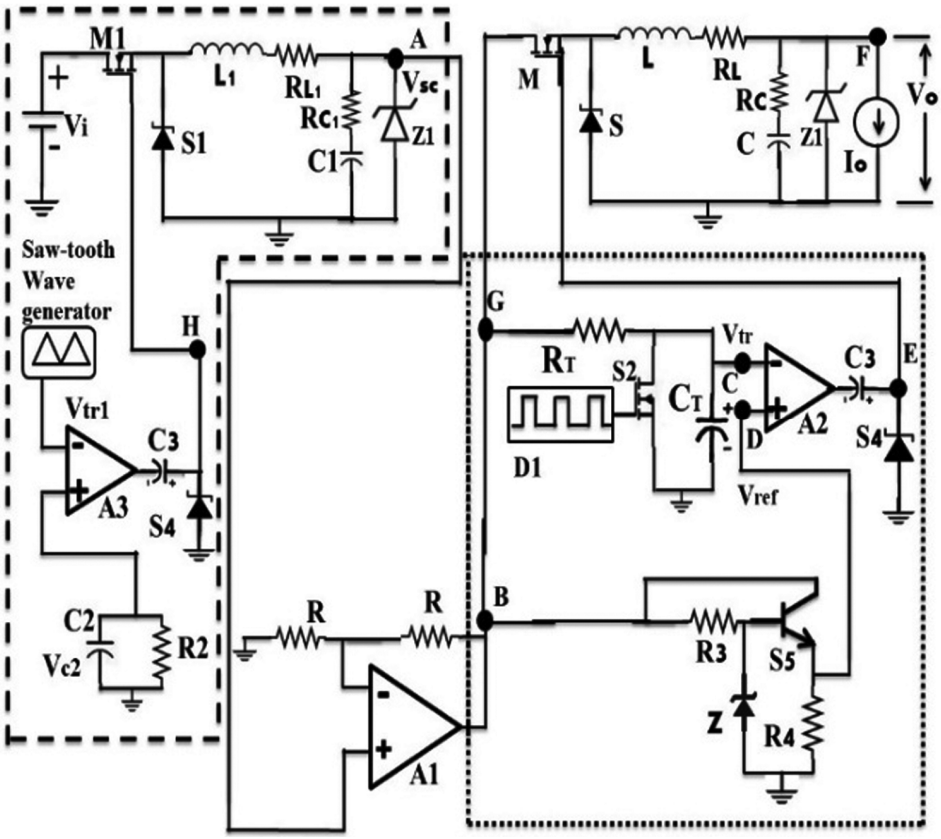

Fig. 2 — The circuit equivalent for SCM discharge powering a constant power application via a buck converter

buck converter, as shown in the circuit given in Fig. 1. A3 is also an op-amp.

The value of 'Vi' is chosen to be almost equal to the initial value of 'VSCM'. 'Vtr1' is the peak voltage of the sawtooth wave that is being used to generate the exponentially decaying duty ratio.

'C2' is a capacitor that is charged at a voltage 'Vc2'. 'Vc2' is taken to be almost equal to 'Vtr1'. 'Vc2' will be decaying at a time constant of 'R2.C2' as the resistance 'R2' is connected to 'C2'. 'Vc2' is the reference voltage being used to generate the exponentially decaying duty ratio. The values of 'R2' and 'C2' are evaluated based on the power consumption of the constant power application to be supplied by SCM via the buck circuit and the power losses in the buck circuit, so that the 'Vc2' and the duty ratio produced using it will decay at the same rate as that of the 'V_{SCM}'. Op-amp A3 is used to compare 'Vtr1' with the decaying 'Vc2', and the output of 'A3' is made unipolar by the circuit made of 'C3' and 'S4' that are connected to the output of 'A3'. As a result, a switching pulse is generated that has a duty ratio decaying exponentially from 1. This duty ratio, along with 'Vi', gives rise to a voltage at point 'A' that decays almost exactly like the voltage of SCM.

The Eq. (1) ensures constant power at a fixed voltage for the application is expressed as follows:

$$\frac{dE_{SCM}}{dt} = C_{SCM} V_{SCM} \frac{dV_{SCM}}{dt} > P_0 \quad \ldots (1)$$

In the Eq. (1), E_{SCM} is the total energy in the SCM at any given time, C_{SCM} is the capacitance of SCM, V_{SCM} is the voltage of SCM, and P_0 is the output voltage of the application being run from SCM via the buck circuit.

This can be further simplified to:

$$\frac{dV_{SCM}}{dt} > \frac{P_0}{V_{SCM} C_{SCM}} \quad \ldots (2)$$

This Eq. (2) implies that the voltage drops across the SCM must satisfy the above relationship, as the SCM serves as an energy source that depletes over time. Consequently, the SCM cannot maintain a constant voltage to the load at the required current for proper operation. To address this, a control loop is necessary to regulate the voltage across the load, ensuring it remains at the desired value while providing the appropriate current.

4 Simulation Results

The components used in the simulation are: MOSFET 2N7000, op-amp LT1360CN8, Schottky diode 1N5819, and Zener diode 1N4732A. 'V_{SCM}=Vi=11.6' and 'C_{SCM}=850 F', 'C2=4700 μF' and 'R2' is a series combination of 25 MΩ, 47 KΩ and 4 Ω.

4.1 Simulation Results for Figure 1

Figure 3 is recorded at point 'A' in Fig. 1. The black line in Fig. 3 represents the decaying voltage of SCM, which is recorded till the peak of the sawtooth wave remains above or equal to the reference voltage of PWM. Up to this point, the load remains connected to the circuit, and hence it will be considered the operation time. The black dashed line in Fig. 3 represents the current supplied by SCM corresponding to the SCM voltage. The current provided by SCM increases as its voltage decreases, allowing for a net constant power to be supplied to the load throughout the operation time. In Fig. 4, the black dashed line represents the peak values

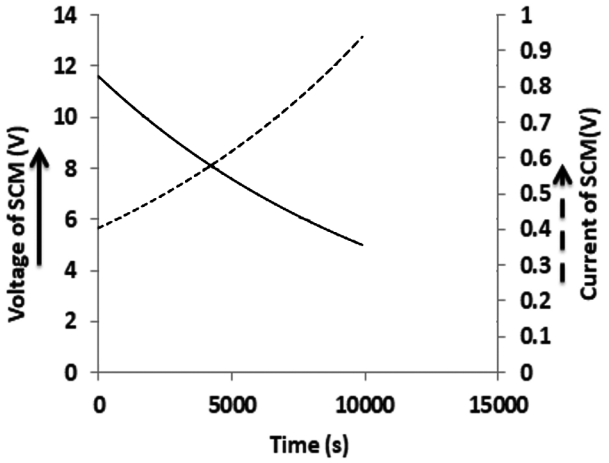

Fig. 3 — Profile of Discharging Supercapacitor Module

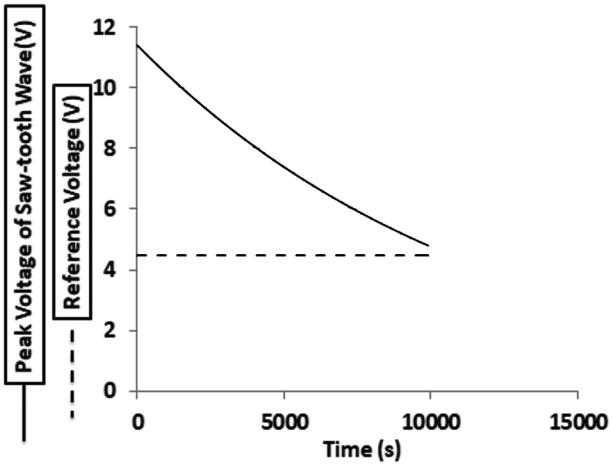

Fig. 4 — Sawtooth Wave Peak Voltage and Reference Voltage

of the sawtooth wave, which are recorded at point 'C' in Fig. 1. The sawtooth wave is generated from the output of op-amp 'A1', and as the output of 'A1' is almost twice the SCM voltage, the peak of the sawtooth wave is also almost equal to twice the SCM voltage. The black line in Fig. 4 represents the PWM reference voltage, which is recorded at point 'D' in Fig. 1. It is maintained at an almost constant value. In Fig. 5, the black line represents the output voltage of the buck circuit in Fig. 1 and is recorded at point 'F' of Fig. 1. An almost steady output voltage is maintained until nearly 10,000 seconds. This will be the operation time until the peak of the sawtooth wave remains above or equal to the reference voltage of the PWM. The black dashed curve in Fig. 5 represents values of duty ratio corresponding to the decaying V_{SCM} and is recorded at point 'E' of Fig. 1, from the graph of duty ratio, it can also be seen that the duty ratio values keep increasing as the V_{SCM} falls while the output voltage is maintained almost constant.

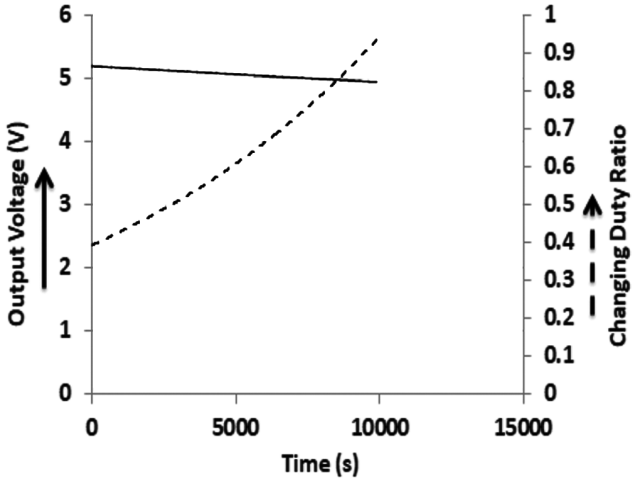

Fig. 5 — Output Voltage and Duty Ratio

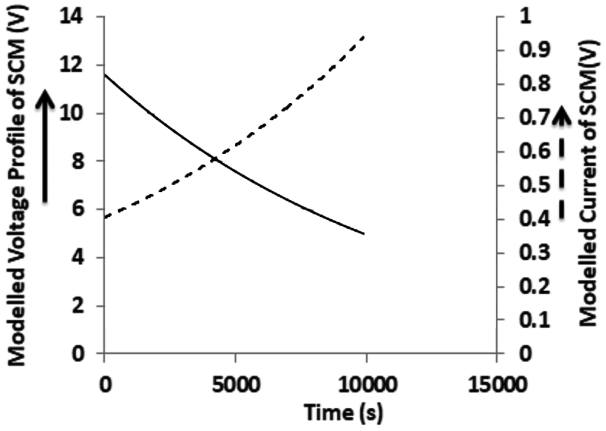

Fig. 6 — SCM Discharge Profile made by Circuit Equivalent for SCM

4.2 Simulation Results for Figure 2

Figure 6 in total represents the characteristics of SCM as emulated by the equivalent circuit for SCM and is obtained at node 'A' of Fig. 2. The black line in Fig. 6 represents the decaying voltage of SCM emulated by the equivalent circuit for SCM, while the dashed line in Fig. 6 represents the current corresponding to the voltage decay behavior of SCM emulated by the equivalent circuit for SCM. In Fig. 7, the black line represents the output voltage of the circuit shown in Fig. 2, which is almost the same circuit as shown in Fig. 1, with the only difference being that now the equivalent circuit for SCM is used in place of the actual SCM to power the same load via the same buck circuit. This output voltage is recorded at node 'F' of Fig. 2. The dashed curve in Fig. 7 is the duty ratio of the switching pulse at point 'H' in Fig. 2. This duty ratio decays from 1 to a certain value, and this duty ratio is used to generate the emulated voltage decay of SCM by decaying the power supply voltage Vi (which ideally should be equal to the starting value of 'V_{SCM}') from V_{SCM} to the certain value in the same way and over the same time as the actual 'V_{SCM}'.

4.3 Comparison of Results

The actual discharge behaviour of SCM displayed in Fig. 3 is found to be almost identical to that of Fig. 6, which is the characteristic of SCM emulated by the power converter. Also, the output voltage of the circuit powered by SCM, indicated by the solid line in Fig. 5, is almost identical to the data given by the solid line in Fig. 7, which is the output voltage of the same circuit powered by the equivalent circuit emulating SCM discharge. So, the equivalent circuit for emulating SCM discharge may be used in place of the actual SCM.

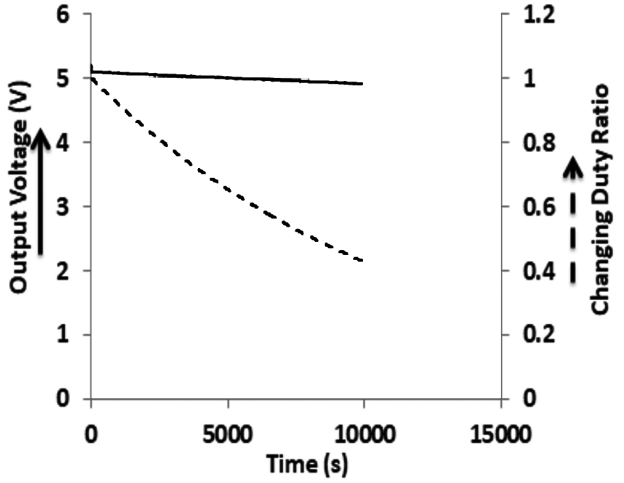

Fig. 7 — Output Voltage and Exponentially Decaying Duty Ratio

5 Experimental Results

The components used in the experiment are MOSFET IRF540N, op-amp LT1360CN8, Schottky diode 1N5819, and Zener diode 1N4732A. 'V_{SCM}' was measured to be 11.34 V, 'Vi' was taken as 12 V and 'C_{SCM}=850 F', 'C2=4700 μF' and 'R2' is a series combination of 2 MΩ, two 400 KΩ, one 27 KΩ, one 10 KΩ and 1KΩ.

5.1 Experimental Results for Figure 1

From Fig. 8, the black solid line is the voltage of SCM with respect to time and is measured at node 'A' of Fig. 1. The dashed line is the respective output voltage of the converter measured at node 'F' of Fig. 1. The output voltage will fall to zero after approximately 156 minutes, as the peak voltage of the sawtooth wave will fall below the reference voltage of the PWM, as observed in Fig. 9.

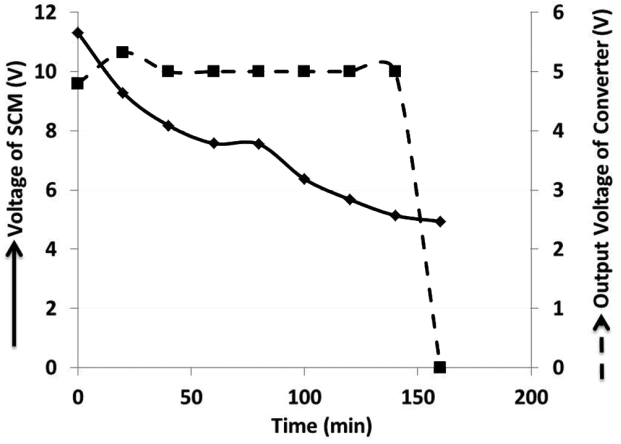

Fig. 8 — Input voltage of SCM and Output Voltage of the converter

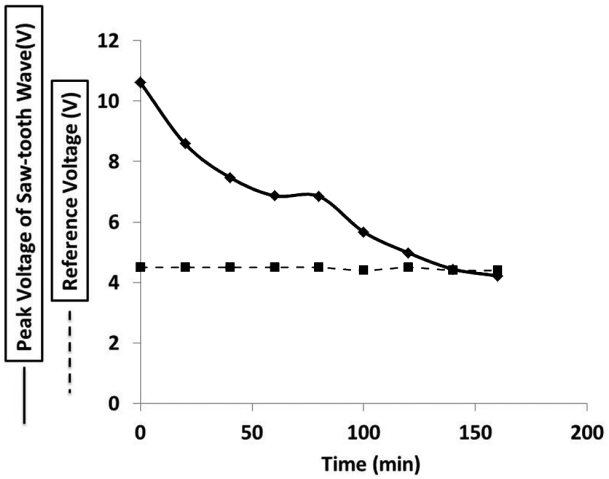

Fig. 9 — Input voltage of SCM and Output Voltage of converter

From Fig. 9, the black solid line curve is the peak value of sawtooth wave for PWM measured at node 'C' of Fig. 1. The black dashed line is the reference voltage of PWM and is measured at node 'D' of Fig. 1.

5.2 Experimental Results for Figure 2

From Fig. 10, the black solid line is a voltage profile similar to the voltage of SCM (modelled voltage of SCM) and is generated using the portion of the circuit in Fig. 2 bordered by dashed lines. This voltage profile is measured at node 'A' of Fig. 2. The black dashed curve in Fig. 10 is the output voltage of the converter when powered by the modelled SCM voltage profile and is measured at node 'F' of Fig. 2.

In Fig. 11, the black dashed curve represents the reference voltage of the PWM converter used to produce a voltage profile like that of a discharging

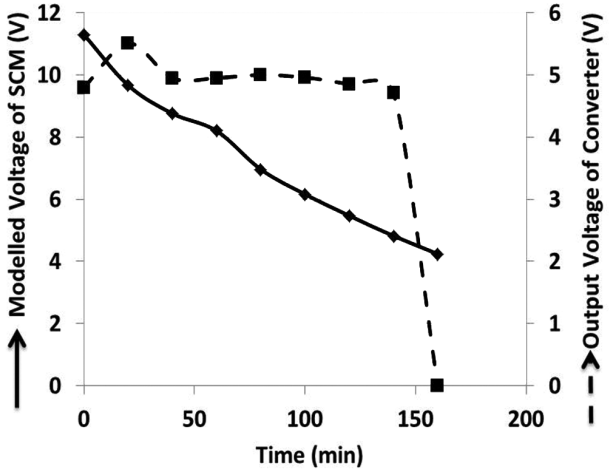

Fig. 10 — Modelled SCM voltage and Output Voltage of the converter

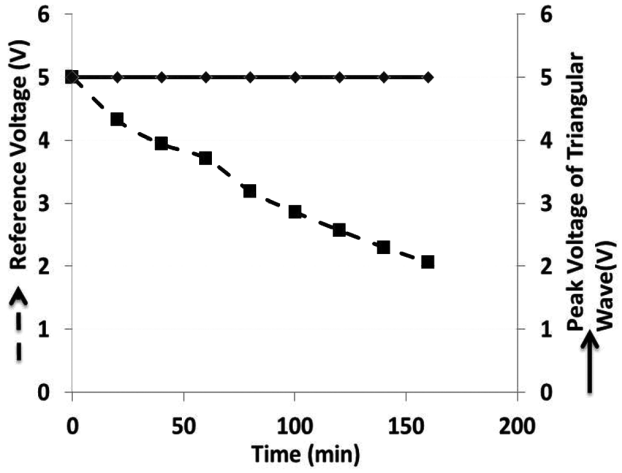

Fig. 11 — Reference Voltage and Peak Voltage of Sawtooth Wave for generating modelled SCM voltage

SCM. This voltage is the voltage of Capacitor C_2 pre-charged to 5V and now discharging under the influence of R_2. This voltage is measured across C_2. The black solid line represents the peak voltage of a constant sawtooth wave at 5V. These two waveforms are compared by op-amp A3 to produce a PWM signal with a decreasing duty ratio.

6 Discussion

If 'E_{SCM}' is the energy supplied from SCM, 'Po' power consumed by the application, 'P_{diss}' is the power dissipated in the ESRs of SCM and 'P_{loss}' is the other cumulative losses in the circuit are given, then the time 't' for which the application would run can be found out using Eq. (3).

$$t = \frac{E_{SCM}}{P_o + P_{diss} + P_{loss}} \quad \ldots (3)$$

$$V_{SCM-final} = V_{SCM-initial} e^{-t/\tau} \quad \ldots (4)$$

$$\tau = R_2 C_2 \quad \ldots (5)$$

$$L = \frac{V_0(1 - D_{min})}{\Delta i_L f_s} \quad \ldots (6)$$

$$C = \frac{\Delta i_L}{8(\Delta V_0) f_s} \quad \ldots (7)$$

This time 't' is also the time needed by the SCM voltage to decay from its initial value '$V_{SCM\text{-}initial}$' to its final value '$V_{SCM\text{-}final}$'. The time constant 'τ' of this voltage decay can be calculated from Eq. (2). After this, the values of R_2 and C_2 are not supposed to be calculated but rather chosen such that Eq. (5) is satisfied, as the product of R_2 and C_2 is the time constant 'τ' for the voltage decay of SCM. Now, these R_2 and C_2 may be used in the portion of the circuit in Fig. 2, inside the black dashed border, to model the discharge behaviour of SCM. For the calculation of other parameters frequency of the switching pulse 'fs' provided to the MOSFET of the buck converter should be known. The other parameters, like inductance value, should be calculated using Eq. (4), and the capacitance value must be chosen to be a value higher than calculated using Eq. (6) as per the reference given [43-44]. The value of 'Δi_L' Eq. (7) should be taken to be 10 % of the output current, and 'ΔV_0' is the amount of ripple to be allowed in the output. 'D_{min}' is the duty ratio corresponding to the highest input voltage for constant output voltage and the lowest output voltage for constant input voltage. This methodology for calculating the operation time of any application running on an SCM is applicable to any SCM of any rating and can also be used to model the discharge characteristic of an SCM.

6.1 Analysis

The model for implementing a DC-DC converter-based circuit that generates the behavior of a discharging supercapacitor has been simulated and verified experimentally. This model does not incorporate temperature dependencies, primarily because it is an RC-based circuit; however, it can be concluded that SCM will discharge at a comparatively faster rate at higher temperatures (45-46). The current model does not deal with the ageing effect on SCM. But it is evident from[47] that ageing of SCM would decrease its effective capacitance to some extent, and the equivalent series resistance (ESR) of SCM should increase linearly. The discharge characteristics are not linear but rather exponential, as evident from both the simulation and experimental results. Thus, nonlinearities are already part of the SCM discharge characteristics. Although the actual discharge characteristics and the modelled characteristic are similar but not exact, to better understand the characteristics, the absolute percentage deviation between the values of voltage of the original supercapacitor characteristic and that modelled using dc-dc converter at different time instants has been graphically shown below:

From Fig. 12, it can be seen that the absolute percentage deviation in values of actual SCM voltage

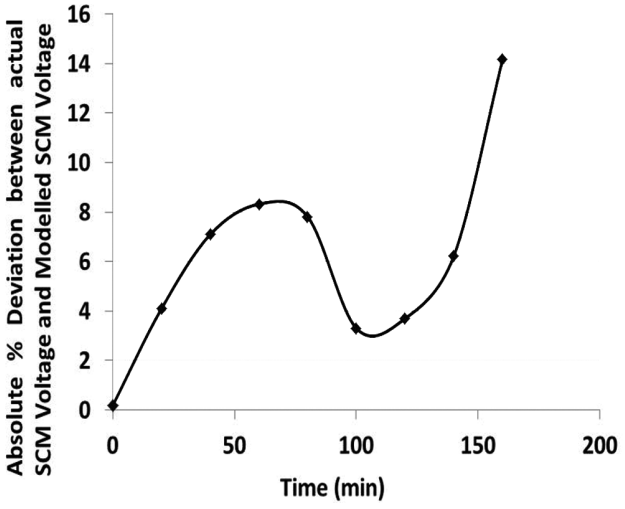

Fig. 12 — Absolute percentage deviation between actual SCM voltage and modeled SCM voltage

Table 1 — Comparative Analysis

Reference Number	Operating Voltage (V)	Capacitance (F)	Power Dissipation Element	Model Build	Load Condition
[36]	2.7	100	8.1 mΩ and 8.7 mΩ	RC based transmission line model	Resistive load
[37]	2.5	110	0.0100478 and 17.4976	two Branch model	no load
	2.5	200	0.0088521 and 8.767		
	2.5	350	0.0048032 Ω and 5.55652 Ω		
	2.7	600	0.002848 Ω and 3.09927 Ω		
[38]	2.7	650	098 mΩ, 2.54 Ω and 43.79 Ω,	Three branch RC model	no load
[39]	2.7	2600	0.5 mΩ	Simulation model	no load
[41]	2.7	3000	290 μΩ	RC model	simple resistive
This Work	11.6	850	0.23 mΩ	Power Electronic model	Constant Power Draw

and modeled SCM voltage ranges between 0.18 % and 14.17 %.

A comparative study can be conducted based on several parameters, such as the basic concept of the work and the methodologies used. In this article, a comparative study is conducted based on the specifications of the supercapacitor used, the type of circuit equivalent, the power dissipation element, and the application type, among others. Only ESR is considered for the power dissipation element. In this work, the SCM is a series combination of four identical supercapacitors, each with a 2.9 V voltage and a 3400 F capacitance, and an ESR of 0.23 mω. The total power dissipation amounts to approximately 0.15 mW. The different parameters based on which comparisons have been made are listed in Table 1. In only one supercapacitor cell, having a capacitance of 100 F and a voltage of 2.7 V, is modelled using an RC-based transmission line model and using a characterization setup, different characteristics of the supercapacitor are found out, and those characteristics are put in a MATLAB Simulink model to get a finalized equivalent model[36]. This is entirely different from the work demonstrated here, in which SCM is used by connecting supercapacitor cells in series. After running a constant power application from this SCM via a buck circuit, the discharge characteristic is determined and eventually modelled using another buck circuit. In the two-branch model, supercapacitors of different specifications are tested, and the values of their power loss elements are determined; however, the equivalent circuit is not used to supply a constant power load[37-38]. An equivalent circuit model for a supercapacitor with a 2.7 V and 650 F rating was developed. The power loss element values in this model were also determined; however, this equivalent model for a supercapacitor has not been used to supply any constant power-drawing load. An RC-based transmission line model for a 2.7 V, 2600 F supercapacitor is designed, and its various parameters are determined for self-discharge analysis. The model is verified using MATLAB and LabVIEW; however, the circuit equivalent has not been verified for load-dependent discharge of supercapacitor[39]. In an RC-based circuit equivalent, a supercapacitor of 2.7 V, 3000 F is modelled, and the equivalent model is shown to be valid only for a resistive load. Based on this, the power loss elements of the equivalent model have been calculated. All the above-described works have no similarity to the work given in this article.

7 Conclusion

For recreating the discharge profile of SCM using a power electronic circuit under different constant power applications as load, an SCM of 850 F and nearly 11.6 to 11.34 V is used to supply a constant power drawing application via a power electronic converter, and the voltage decay characteristic of SCM is recorded in Fig. 3 along with the output voltage of the converter circuit which is given in Fig. 5. Thereafter, the operation time, as determined from the simulation results in Fig. 2, and the time constant of voltage decay are estimated mathematically using Eqs. (1) and (2). Then, a combination of resistance and capacitance values is chosen for the time constant, and this combination is used in the PWM switching circuit of another buck topology, which uses the battery as input, as shown in Fig. 2. This Buck topology is used in place of the SCM

as the source to power the entire circuit of Fig. 1. The SCM voltage decay modelled by the circuit equivalent of SCM (shown by the portion of the circuit in Fig. 2 bordered by black dashed lines) is recorded in Fig. 6. It has been found to closely match the actual voltage decay characteristic of SCM, as shown in Fig. 3. The output voltage of the circuit in Fig. 1 (Given by a black line in Fig. 5) is found to be almost identical to the output voltage of the circuit given in Fig. 2 (given by a black line in Fig. 7). Also, the operating time is almost 2 hours and 45 minutes. Hence, it can be concluded that the circuit equivalent of SCM can be used as a test circuit in place of the SCM to supply a constant power application, and the different parameters, like circuit operation time, etc., can be accurately estimated, especially because the output voltages of both circuits in Figs. 1-2 are found to be almost identical. The experimental results further validate the model, as the output voltage of the converter is almost identical (Figs. 8 and 10) for both cases: when the converter is powered from the SCM and when it is powered from the modelled voltage of the SCM. Although there is a deviation in the actual voltage profile of SCM (Fig. 8) and the one modelled using a DC-DC converter (Fig. 10), the absolute % deviation in values is quite small, with the highest being approximately 14.17 %.

References

1 Reddy T S, Junaid K A, Sukhi Y, Jeyashree Y, Kavitha P & Nath V, *Adv Electr Eng Electron Energy*, 5 (2023) 100206.

2 Junaid K A, Sukhi Y, Anjum N, Jeyashree Y, Ahamed A F, Nath V, Debbarma S, *et al*., *Adv Electr Eng Electron Energy*, 5 (2023) 100271.

3 Wang S, Wei T & Qi Z, *Proceed ISES World Congress 2007 Springer Berlin Heidelberg,* 1 (5) (2008) 2805.

4 Kinjo T, Senjyu T, Urasaki N & Fujita H, *IEEE Trans Energy Conver*, 21 (2006) 221.

5 Zhang Z, Zhang X, Chen W, Rasim Y, Salman W, Pan H & Wang C, *Appl Energy*, 178 (2016) 177.

6 Bhatia C M, Banga S, Khurana M, Malhotra S, Juneja B, Bhardwaj H & Kapahi M, *IETE Tech Rev*, 23 (2006) 321.

7 Hasanpour S, Baghramian A & Mojallali H, *IEEE Trans Power Electron*, 35 (2020) 8088.

8 Neto P B, Saavedra O R & De Souza Ribeiro L A, *IEEE Trans Sustain Energy*, 9 (2018) 1618.

9 Ganesan S, Subramaniam U, Ghodke A A, Elavarasan R M, Raju K & Bhaskar M S, *IEEE Access*, 8 (2020) 188861.

10 Hamajima T, Amata H, Iwasaki T, Atomura N, Tsuda M, Miyagi D & Kajiwara M, *IEEE Trans Appl Superconduct*, 22 (2012) 5701704.

11 Aneke M & Wang M, *Appl Energy*, 179 (2016) 350.

12 Malamaki K-N D, Casado-Machado F, Barragan-Villarejo M, Gross A M, Kryonidis G C, Martinez-Ramos J L & Demoulias C S, *IEEE Trans Industry Appl*, 58 (2022) 7581.

13 Becker H I, *General Electric Co*, *USA*, (1957) 2800616.

14 Shylashree N, Amulya M S, Disha G R, Praveena N, Verma V K, Muthumanickam S & Nath V, *IETE J Res*, 1 (2023).

15 D Arnaudov N H, *19th International Symposium on Electrical Apparatus and Technologies (SIELA)*, *Bourgas, Bulgaria*, 1 (2016).

16 Sengupta A S, Satpathy S, Mohanty S P, Baral D & Bhattacharyya B K, *IEEE Consumer Electron Mag*, 7 (2018) 50.

17 Rocabert J, Capo-Misut R, Munoz-Aguilar R S, Candela J I & Rodriguez P, *IEEE Trans Industry Appl*, 55 (2019) 1853.

18 Roy P, He J & Liao Y, *IEEE Access*, 8 (2020) 210099.

19 Kollimalla S K, Mishra M K & Narasamma N L, *IEEE Trans Sustain Energy*, 5 (2014) 1137.

20 Camara M B, Gualous H, Gustin F, Berthon A & Dakyo B, *IEEE Trans Industrial Electron*, 57 (2010) 587.

21 Kazerani A O, *IEEE Trans Vehicular Technol*, (2015) 4449, doi: 10.1109/TVT.2014.2371912.

22 Simjee F I & Chou P H, *IEEE Trans Power Electron*, 23 (2008) 1526.

23 Sengupta A S, Chakraborty A K & Bhattacharyya B K, *IETE J Res*, 66 (2018) 115.

24 Sengupta A S, Mohanty S P & Bhattacharyya B K, *IET Power Electron*, 11 (2018) 1946.

25 Padhee S, Pati U C & Mahapatra K, *IETE Tech Rev*, 35 (2016) 99.

26 Cornea O, Hulea D, Muntean N & Andreescu G-D, *IEEE Access*, 8 (2020) 136092.

27 H Antchev A A, *In Proceedings 17th Conference on Electrical Machines, Drives and Power Systems (ELMA), Sofia, Bulgaria,* (2021) 1, doi: 10.1109/ELMA52514.2021.9502967.

28 Zhou G, Xu J & Wang J, *IEEE Trans Industrial Electron*, 61 (2014) 1280.

29 Xu J & Qin M, *IET Power Electron*, 3 (2010) 391.

30 Chung J -E-M, *IEEE Electron Device Lett*, 44 (10) (2023) 1792.

31 R M Reddy M D, *IEEE Trans Circuits Syst II*, 70 (7) (2023) 2580.

32 Zubieta L & Bonert R, *IEEE Trans Industry Appl*, 36 (2000) 199.

33 Gualous H, Bouquain D, Berthon A & Kauffmann J M, *J Power Sources*, 123 (2003) 86.

34 Fletcher S, Black V J & Kirkpatrick I, *J Solid State Electrochem*, 18 (2013) 1377.

35 Umanand L, Power Electron Essential Appl, *Wily India Pvt. Ltd*, 1st Edn, (2009).

36 Logerais P O, Camara M A, Riou O, Djellad A, Omeiri A, Delaleux F & Durastanti J F, *Int J Hydrogen Energy*, 40 (2015) 13725.

37 Faranda R, *Electric Power Syst Res*, 80 (2010) 363.

38 Liu K, Zhu C, Lu R & Chan C C, *IEEE Trans Plasma Sci*, 41 (2013) 1267.

39 Kim S-H, Choi W, Lee K-B, & Choi S, *IEEE Trans Power Electron*, 26 (2011) 3377.

40 Chai R, & Zhang Y, *IEEE Trans Power Electron*, 30 (2015) 6720.

41 Liu C, Wang Y, Chen Z & Ling Q, *J Power Sources*, 374 (2018) 121.

42 Pourkheirollah H, Keskinen J, Mäntysalo M & Lupo D, *IEEE Trans Power Electron,* 535 (2022) doi:10.1016/ j.jpowsour.2022.231475.

43 Hauke B, *Texas Instr*, Application Report SLVA477B Rev, (2015).

44 Xiong G, Kundu A & Fisher T S, *Springer Briefs in Thermal Engineering and Applied Science*, DOI 10.1007/978-3-319-20242-6_4
45 K¨ops L, Kreth F A, Klein M & Balducci A, *J Power Sources*, 581 (2023), doi.org/10.1016/j.jpowsour.2023.233480.
46 Sedlakova1 V, Sikula1 J, Majzner J, Sedlak1 P, Kuparowitz T, Buergler B & Vasina P, *Metrol Measure Syst*, 23 (2016), DOI: 10.1515/mms-2016-0038.
47 Anjum N, Yadav V K S & Nath V, *IJMIT*, 1 (2) (2023) 82.
48 Suman P N, Kumari J, Anjum N, Kiran A, Muthumanickam S, Rai A, Debbarma S, Kumar S, Ojha M K, Nath V & Mishra G K, *IETE J Res*, (2024) 1, https://doi.org/10.1080/03772063.2024.2307426
49 Anjum N, Yadav V K S & Nath V, *Ind J Pure Appl Phys*, 63 (6) (2025) 517.
50 Sharma D & Nath V, *Circuits Syst Signal Process*, 44 (2025) 2266.
51 Reddy S T & Nath V, *Sci Rep*, 15 (2025) 9585.
52 Sharma D & Nath V, *Analog Integr Circ Sig Process*, 122 (2025) 39.